Localization of Multidrug Transporter Substrates within Model Membranes†

Alena Siarheyeva, Jakob J. Lopez, and Clemens Glaubitz*

Centre for Biomolecular Magnetic Resonance and Institute for Biophysical Chemistry, J. W. Goethe Universität, Max-von-Laue Strasse 9, D-60438 Frankfurt, Germany

Received December 6, 2005; Revised Manuscript Received February 15, 2006

ABSTRACT: Active extrusion of drugs from the cell interior by primary and secondary efflux pumps is an essential mechanism underlying the phenomenon of multidrug resistance. The first discovered and best characterized primary efflux pump found in humans is the ABC transporter P-glycoprotein (PGP), which shows very broad substrate specificity. Many of these molecules are lipophilic, and binding most likely takes place within the membrane. PGP could either translocate them from the inner to the outer leaflet (flippase) or extrude them from the membrane into the extracellular environment (hydrophobic vacuum cleaner). Recognition and binding of such a diverse set of substrates must be associated with a preferred membrane location, determined by molecular properties and lipid interactions. Therefore, a systematic study of the interaction among seven PGP substrates (phenazine, doxorubicin, cephalexin, ampicillin, chloramphenicol, penicillin G, and quercetin) and two modulators (quinidine and nicardipine) and 1,2-dimyristoyl-*sn*-glycero-3-phosphocholine (DMPC) model membranes is reported here. The location profile of these molecules across the membrane was determined by ^{1}H NOESY MAS NMR based on ^{1}H−^{1}H cross-peaks between their aromatic fingerprint region and lipid resonances. Although structurally rather diverse, all tested substances are found to have their highest concentration between the phosphate of the lipid headgroup and the upper segments of the lipid hydrocarbon chains. Our findings are consistent with PGP substrate and modulator binding from the membrane interface region.

The development of resistance to multiple drugs is a major problem in the treatment of a number of infectious diseases and cancer. The phenomenon of multidrug resistance is based on the synergistic interplay of different mechanisms, such as target inactivation, target alteration, prevention of drug influx, and active extrusion of drugs from the cell (*1*). The latter is mediated by overexpression of multidrug efflux pumps. Almost all known antibiotics, especially those that are small in size (FW < 1000) and partially hydrophobic in character, can be targeted by multidrug efflux pumps (*2*). An increasing number of multidrug transporters have been identified in human cells, bacteria, and yeast (*2*). Their importance is illustrated by the fact that they constitute ∼6−18% of all transporters in microbial cells (*3*).

The mammalian plasma membrane transporter P-glycoprotein (PGP)[1] was the first discovered and is so far the best characterized multidrug efflux pump (*4*). It is a member of the ATP binding cassette (ABC) superfamily and acts as an active transporter for a variety of anticancer agents, using the energy released by ATP hydrolysis (*5*). Interestingly, a very similar protein has also been found in bacteria. LmrA from *Lactococcus lactis* not only possesses a high degree of sequence similarity with PGP but also shares remarkably a similar substrate specificity (*6*).

The translocation of drugs could be accomplished by a transporter acting as a "classical pump", as a "flippase", or as a "hydrophobic vacuum cleaner". A flippase mechanism requires the drugs to enter the inner membrane leaflet, where they bind to the protein, which subsequently flips the compounds to the outer leaflet. From there, they could diffuse into the extracellular space as proposed for phosphatidylcholine transport (*5*). The vacuum cleaner model suggests that drugs diffuse into the lipid phase from which they enter the protein which expels them through a proposed central channel (Figure 1) (*7*, *8*). Both models require substrate accumulation within the membrane in contrast to the classical pump mechanism. A classical pump, in which the transporter takes up drugs from the aqueous phase and translocates them into extracellular space, seems unlikely, as it has been clearly demonstrated that substrates enter the protein from the membrane as outlined below.

During the transport cycle, substrates bind first to a high-affinity binding site and are released subsequently from a low-affinity binding site (*9*, *10*). To map these PGP binding sites, various amino acid substitutions, cysteine mutagenesis coupled with cross-linking, and photoaffinity labeling studies have been carried out (*9*, *11*−*14*). These experiments identified residues in transmembrane helices 4−6 and 8−12 as well as in the loops and the ATP binding cassette as being important for substrate binding and/or transport. It has been

† This research was supported by SFB 628 'Functional Membrane Proteomics'. A.S. acknowledges a scholarship from the International Max Planck Research School Frankfurt for Membrane Biophysics.

* To whom correspondence should be addressed. Telephone: +49 69798 29927. Fax: +49 69798 29929. E-mail: glaubitz@em.uni-frankfurt.de.

[1] Abbreviations: PGP, P-glycoprotein; DMPC, 1,2-dimyristoyl-*sn*-glycero-3-phosphocholine; DMPG, 1,2-dimyristoyl-*sn*-glycero-3-[phospho-*rac*-(1-glycerol)]; NOESY MAS NMR, magic angle spinning nuclear Overhauser enhancement spectroscopy; ABC transporter, ATP binding cassette transporter; MDR, multidrug resistance; TMA-DPH, diphenylhexatriene derivative; egg PC, egg phosphatidylcholine; brain PS, brain phosphatidylserine; egg PE, egg phosphatidylethanolamine.

10.1021/bi0524870 CCC: $33.50
Published on Web 04/18/2006

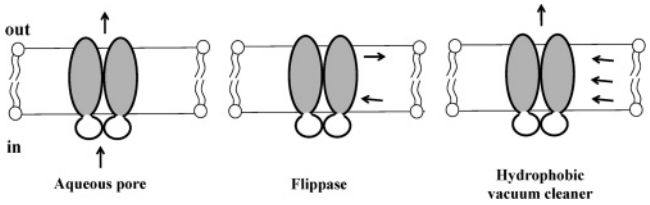

FIGURE 1: Multidrug efflux pumps could either translocate substrates through an aqueous pore, flip lipophilic substrates from one leaflet to the other, or collect them from any part in the membrane and release them into the extracellular space.

suggested on the basis of these data that the PGP drug-binding domain is a large, flexible "funnel" which narrows at the cytoplasmic side. Moreover, it has been proposed that different substrates can have overlapping binding sites within this large binding pocket (*4*, *9*). In contrast, several experiments using fluorescent PGP substrates [for example, diphenylhexatriene derivative (TMA-DPH) and Hoechst-33342] have been performed, mapping the binding site locations close to the membrane boundary of the cytoplasmic leaflet (*15*, *16*). Resolving the controversy about the location of the drug binding site(s) would help in the constuction of a consistent model of the ABC MDR efflux pump transport cycle.

Many experimental hints suggest that aromatic residues in PGP are involved in substrate binding, and it has been proposed that van der Waals forces, $\pi-\pi$ stacking interactions, electrostatic forces, the hydrophobic effect, and, to a lesser extent, a hydrogen-bonding component contribute to the substrate binding of multidrug transporters (*4*, *17*). The nature of drug binding is to some extent also influenced by drug−lipid interactions. The transport models described above and the membrane-based location of a binding pocket are consistent with the hydrophobicity of many substrates, determined from their *n*-octanol−water partition coefficient. However, these partition coefficients are only of limited value as phospholipid bilayers are not homogeneous hydrophobic two-dimensional solvents but contain partially ordered hydrocarbon chains between highly ordered, charged headgroup regions. If structurally diverse molecules exhibit a similar interaction pattern within membrane lipids, a common binding site could be envisaged, as all substrates would be located in the same region within the membrane. In contrast, if each substrate behaves differently, a larger, less specific binding pocket within the membrane would be required.

Questions concerning the binding site and transport models described above and the lack of information about substrate−membrane interactions have motivated the experiments described here. We present a systematic NOESY MAS NMR study on selected samples, with the goal of determining the location of a set of PGP substrates and modulators within phospholipid bilayers.

Cells overexpressing PGP have been shown to possess an increased resistance to at least eight classes of clinically relevant broad-spectrum antibiotics, including aminoglycosides, lincosamides, macrolides, quinolones, streptogramins, tetracyclines, and chloramphenicol, which are neutral or positively charged hydrophobic compounds (*4*). Although it is difficult to define common specific chemical features of these substrates, most of them can be characterized by at least one planar aromatic domain, often a basic nitrogen atom within a nonaromatic moiety. In most cases, they are positively charged or neutral under physiological conditions (*9*, *18*−*20*). Interestingly, it is the neutral form of the drugs which diffuses faster across the membrane and which is preferably transported by PGP as shown for anthracyclines (*21*).

Table 1: PGP Substrates Used in This Study and Their Octanol−Water Partition Coefficients (log P_{ow})[a]

molecule	category	log P_{ow}
A, phenazine	miscellaneous	2.8 ± 0.3
B, doxorubicin	anthracyclines	2.3 ± 0.7
C, cephalexin	bacteriostatic	0.6 ± 0.3
D, ampicillin	bacteriostatic	1.3 ± 0.3
E, quinidine	antimalarial PGP modulator	3.4 ± 0.4
F, chloramphenicol	bacteriostatics	1.0 ± 0.3
G, nicardipine	calcium channel blockers, PGP modulator	5.2 ± 0.6
H, penicillin G	bacteriostatic	1.7 ± 0.2
I, quercetin	bacteriostatic	2.2 ± 1.0

[a] Data are estimates (*72*) and were obtained via SciFinder Scholar (Chemical Abstracts Service).

The nine substrates used in this study are listed in Table 1 together with their octanol−water partitioning coefficients (log P_{ow}). Their chemical structures are given in Figure 2. They have been shown to act as either substrates or modulators for PGP and LmrA (*4*, *9*, *22*) and belong to distinct drug classes such as Ca^{2+} channel blockers, anthracyclines, cytotoxic agents, antihypertensives, or bacteriostatics.

The influence of the lipid environment on the binding affinity has been studied for a number of substrates by fluorescence quenching on reconstituted PGP (*23*). It was found that the affinity is highest for egg PC and DMPC, followed by those for brain PS and egg PE. As DMPC has been well-characterized by solid-state NMR, we have selected it for this study as a model membrane matrix for all nine drugs. To our knowledge, only four of the nine substrates used here have been investigated before with respect to their membrane interaction. Their location within the membrane has never been determined.

So far, insight into drug location and interaction with membranes has relied on calorimetry (*24*), molecular modeling (*25*), ^{1}H, ^{14}N, and ^{31}P NMR spectroscopy (*26*, *27*), $^{1}H-^{13}C$ dipolar coupling constants (*26*, *28*), ^{2}H order parameters (*29*, *30*), and fluorescence measurements (*29*, *31*). MAS-NOESY (magic angle spinning assisted nuclear Overhauser enhancement spectroscopy) has been shown by Gawrisch and co-workers to be a powerful tool in studying the distribution of the substrate within model lipid bilayers in multilamellar dispersions (*32*−*34*). It was found that NOE cross-peaks between lipid resonances arise mainly from inter- rather than intramolecular interactions due to the anisotropic nature of molecular motions in membrane bilayers (*35*). Therefore, NOEs between substrate and lipid resonances could serve as a measure of substrate distribution within the membrane surfaces. Indeed, using MAS-NOESY, the distribution of ethanol in model lipid membranes (*34*), the location of anesthetics and hydrophobic ions in liposomes (*36*, *37*), the preference of flavonoids and tryptophan for the membrane interface (*27*, *33*), and the interaction of a peptide (*32*) have been investigated in the past. Here, we have used the protons located in the aromatic rings of all nine molecules as a spectral fingerprint and molecular reporter to determine their location probability within the membrane.

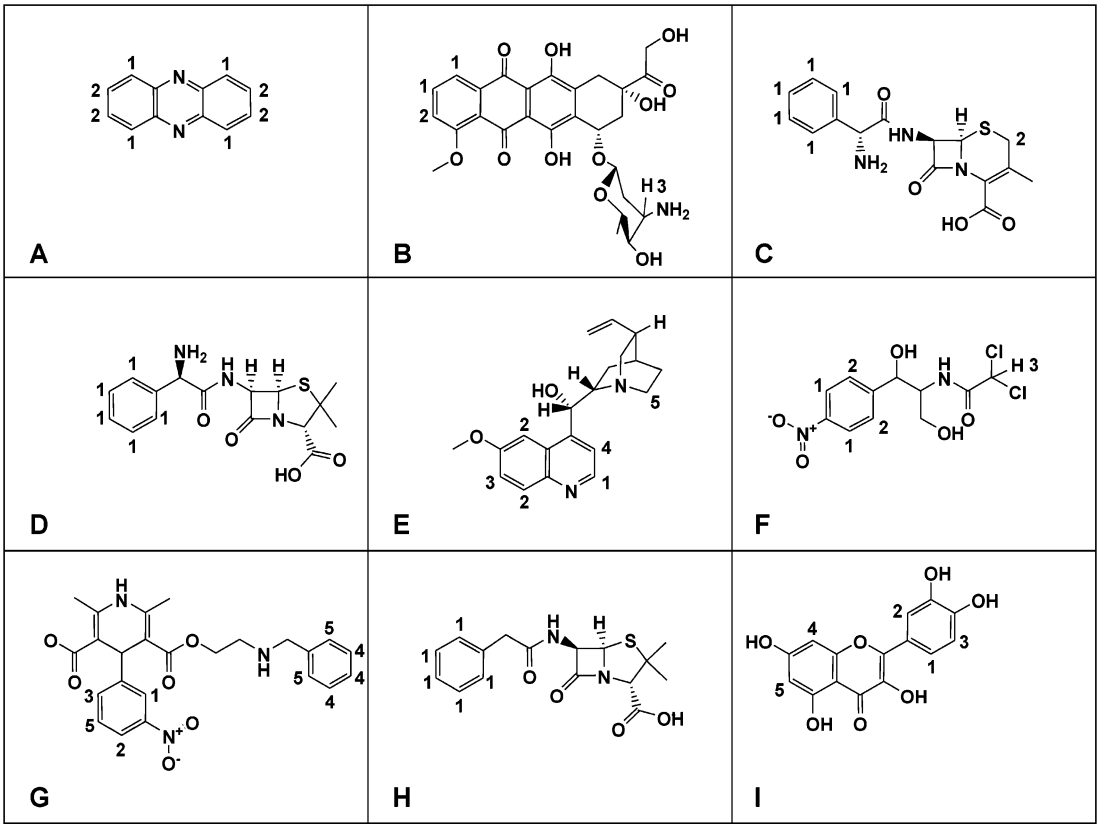

FIGURE 2: Chemical structures of P-glycoprotein substrates used in this study: (A) phenazine, (B) doxorubicin, (C) cephalexin, (D) ampicillin, (E) quinidine, (F) chloramphenicol, (G) nicardipine, (H) penicillin G, and (I) quercetin. Classifications and partition coefficients are given in Table 1.

To study substrate−lipid interactions, we used a "single-mixing time approximation" (*35*). This approximation has served reliably in the past, but to ensure that the results of this approach are indeed realistic, we compared them to those obtained using a full cross-relaxation rate matrix analysis from a series of NOESY cross-peak buildup curves, as described below.

EXPERIMENTAL PROCEDURES

Materials. The phospholipids 1,2-dimyristoyl-*sn*-glycero-3-phosphocholine (DMPC) and 1,2-dimyristoyl-*sn*-glycero-3-[phospho-*rac*-(1-glycerol)] (DMPG) were obtained from Sigma. Penicillin G was obtained from Fluka BioChemika and ampicillin from Roth. All other reagents were purchased from Sigma.

Sample Preparation. Substrates and DMPC (ca. 25 mg) were dissolved separately in 2 mL of chloroform and methanol (1:1) and mixed. The drug:lipid molar ratios were as follows: 0.28 for phenazine, 0.22 for doxorubicin, 0.22 for cephalexin, 0.22 for quinidine, 0.22 for penicillin G, 0.22 for quercetin, 0.18 for ampicillin, 0.26 for chloramphenicol, and 0.27 for nicardipine. The solvent was removed under a stream of nitrogen. The lipid film was redissolved in 2 mL of cyclohexane, frozen in liquid nitrogen, and lyophilized under vacuum overnight. Multilamellar vesicles were prepared by hydrating each sample with approximately 20 μL of pure D_2O. The samples were homogenized by 5−10 freeze−thaw cycles. The pellet was transferred to a 4 mm MAS rotor. Before data were acquired, the sample was spun at 8 kHz in the MAS rotor for 15 min to allow for homogeneous sample distribution and temperature equilibration. To study the charged forms of some of the drugs, samples were buffered at pH 7.4 (10 mM Tris and 50 mM KCl).

NMR Measurements. NMR experiments were performed on a Bruker Avance 400 instrument equipped with a 4 mm MAS probe at 300 K, ensuring that DMPC is maintained in the liquid crystalline phase. All ^{1}H experiments were carried out at a resonance frequency of 400.131 MHz, with a spectral width of 8 kHz. The sample was spun at 8 kHz. Inserts made of Kel-F were used to keep the samples centered within the 4 mm zirconium MAS rotor. Two-dimensional NOESY experiments were acquired in phase sensitive mode with 90° pulses of 3 μs. A total of 256 complex data points were collected in the indirect dimensions with 16 transients per increment with a delay of 4 s between scans. A squared sine-bell window function was applied in both dimensions before processing. All ^{1}H spectra were referenced with respect to the terminal methyl group of the lipid chains at 0.89 ppm of a DMPC sample in the absence of drug molecules.

Data were processed using XWIN NMR (Bruker Instruments, Karlsruhe, Germany). NOESY cross-peak volumes were obtained by integration using the software packages Sparky (T. D. Goddard and D. G. Kneller, SPARKY 3, University of California, San Francisco) and CARA (R. Keller, www.nmr.ch). Data handling, calculations, and fitting were done with the help of the open source software packages Tcl/Tk (B. B. Welch, http://dev.scriptics.com), GNU OCTAVE (version 2.1.71, http://www.octave.org), and GNUPLOT (version 4.0, T. Williams and C. Kelley, http://www.gnuplot.info).

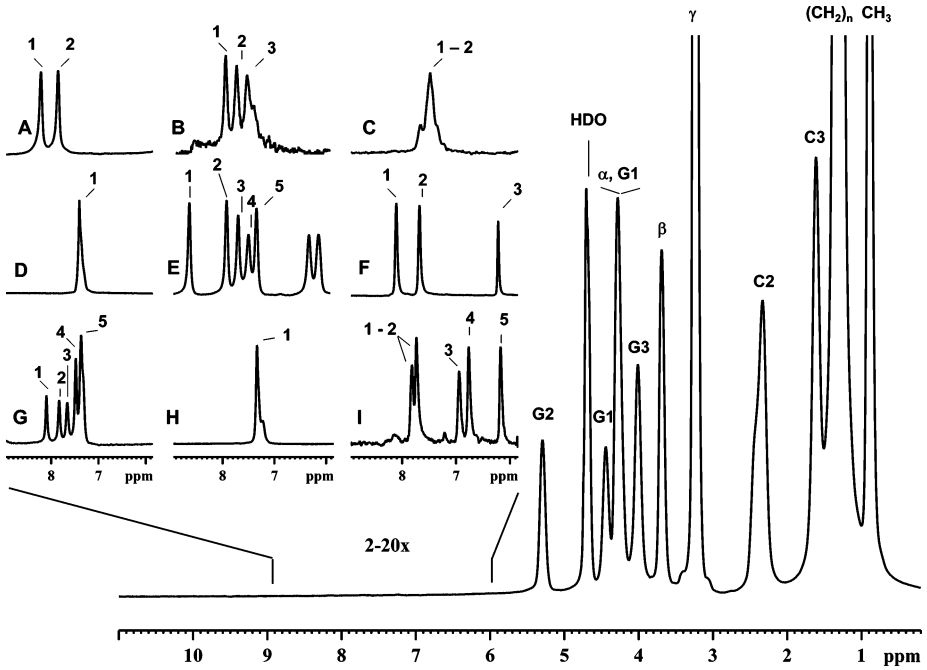

FIGURE 3: ^{1}H MAS NMR spectra (400 MHz) of DMPC/D_2O dispersions containing nine different substrates and modulators taken at a spinning rate of 8 kHz and 300 K. Lipid resonances are labeled according to the assignment shown in Figure 5. The proton spectra of drug/lipid samples are plotted from 6 to 9 ppm: (A) phenazine (*73*), (B) doxorubicin (*74*), (C) cephalexin (*40*), (D) ampicillin (*40*, *75*), (E) quinidine (*45*), (F) chloramphenicol (*41*), (G) nicardipine (*42*), (H) penicillin G (*40*), and (I) quercetin (*27*).

To ensure that the single mixing time approximates the cross-relaxation rates between protons in the aromatic groups of the substrates and in the lipids, a comparison was made with a two-spin approximation and a full relaxation matrix approach. The two-spin method takes into account the interactions between just two nuclei while ignoring the effect of others within the dipolar coupling range (*35*). All three methods were evaluated by comparing the results from a set of spectra obtained from quinidine in DMPC.

NOESY spectra for the DMPC/quinidine mixture were acquired for eight mixing times, ranging between 10 and 1000 ms. The distribution profiles of the ligand within the lipid matrix, calculated with the full relaxation matrix method, two-spin approximation, and single-mixing time equation, were qualitatively very similar (see the Supporting Information). This is not surprising, as Gawrisch and coworkers have demonstrated that the cross-relaxation rates or in other words cross-peak volumes (normalized with respect to the number of lipid protons contributing to cross relaxation) obtained from a single-mixing time MAS-NOESY experiment are sufficient for characterizing lipid−lipid and subsequently lipid−substrate interactions (*34*, *35*). Therefore, for all nine substrates, the location probability was estimated from data obtained at only one mixing time (*35*), which is most convenient in terms of time and effort:

$$\sigma_{ij} = \frac{A_{ij}(t_m)}{A_{jj}(t_m) \times t_m}$$

The cross-relaxation rate (σ_{ij}) is estimated by dividing the cross-peak volume (A_{ij}) by the diagonal peak volume (A_{jj}), multiplied by the mixing time (t_m) of the NOESY spectrum.

RESULTS

Although the drugs in this study vary in molecular size and structure, a common feature is the occurrence of aromatic moieties in each molecule (Figure 2), which seem to be directly involved in protein binding (*38*, *39*). The NMR signals of the aromatic protons are well-resolved and well-separated from dominating lipid resonances, as shown in Figure 3 for all nine molecules, a fact which makes these groups ideal probes for substrate−lipid interactions. The ^{1}H chemical shift assignments of substrates and synthetic lipid DMPC have been determined before and are shown in Figures 2 and 5 (*40*−*45*).

Figure 4 shows the two-dimensional MAS NOESY spectra for quinidine/DMPC and penicillin G/DMPC vesicles at a mixing time of 400 ms. The cross-peaks indicating intermolecular drug−lipid interactions are highlighted. Interactions are found with almost every lipid resonance, in agreement with the expected penetration of the drug into the lipid bilayer.

The cross-relaxation rates correspond to the amount of magnetization transfer between drug and lipid protons and give a measure of the frequency of collisions between both molecules. In the single-mixing time approximation, cross-relaxation rates are proportional to normalized cross-peak volumes. By plotting these values for each cross-peak as a function of the corresponding lipid proton location within the membrane, we obtain a distribution of the drug across the membrane. The results of our measurements are shown in Figure 5 for one representative proton selected from each substrate. Normalized cross-peak volumes are plotted from the hydrophobic core of the membrane to the headgroup region from left to right, respectively. None of the substrates shows a strong correlation with the hydrophobic core region. Interestingly, all resolved substrate protons shown in Figure 3 feature a similar location profile (see the Supporting Information). Our data show that the aromatic groups of all studied molecules follow a general pattern of preferred equilibrium in a layer located below the headgroup phosphate and above the first segments of the lipid acyl chain.

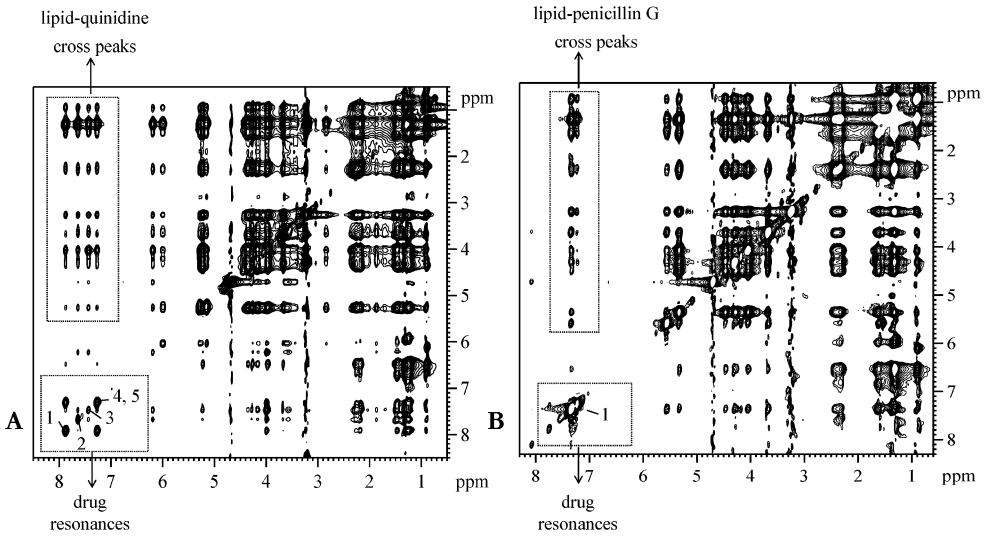

FIGURE 4: Examples for two-dimensional ^{1}H MAS NMR NOESY spectra of quinidine (A) and penicillin G (B) DMPC dispersions in D_2O recorded with a mixing time of 400 ms at 300 K. Both spectra show intense cross-peaks between drugs and DMPC resonances.

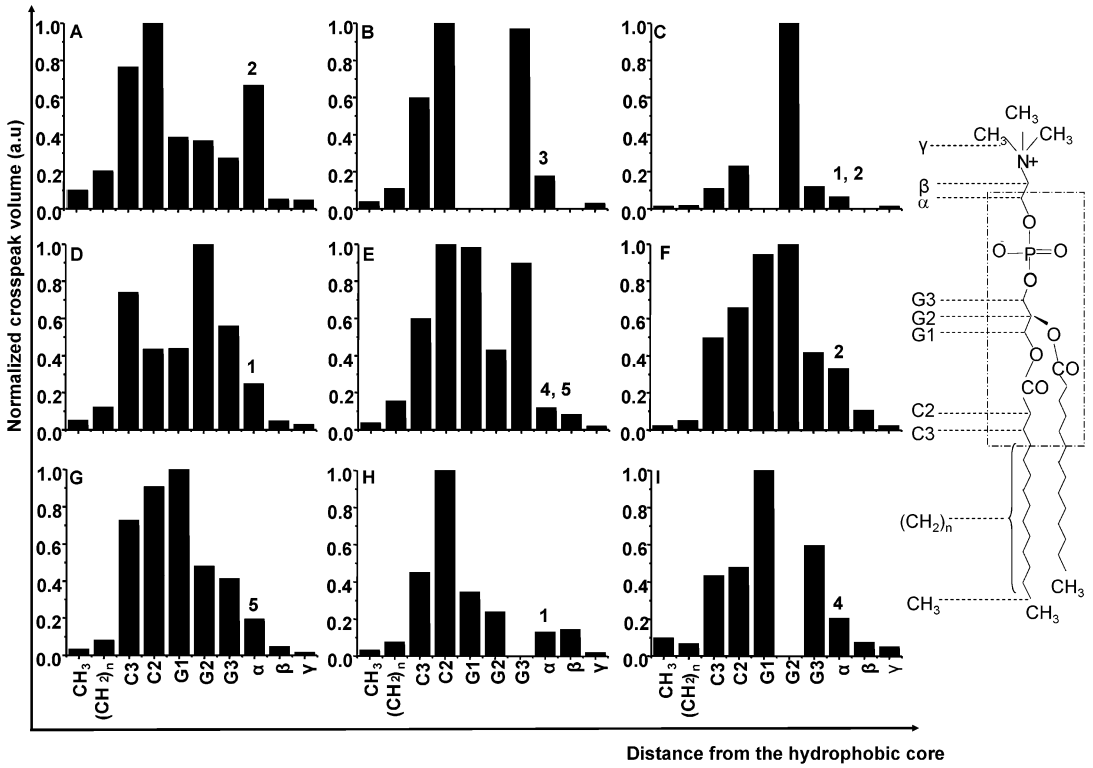

FIGURE 5: Following the single-mixing time analysis (see the text for details), normalized DMPC−substrate cross-peak volumes for selected aromatic protons according to the ^{1}H assignments in Figures 2 and 3 are plotted in the order of increasing distance from the hydrophobic core of the membrane. For all drugs, a high location probability is observed between lipid chain segment C3 and headgroup segment α: (A) phenazine, (B) doxorubicin, (C) cephalexin, (D) ampicillin, (E) quinidine, (F) chloramphenicol, (G) nicardipine, (H) penicillin G, and (I) quercetin. DMPC proton assignments are shown at the right: $N(CH_3)_3$ (γ), N-$\underline{CH_2}$-CH_2 (β), CH_2-$\underline{CH_2}$-O (α), O-$\underline{CH_2}$-CH (G3), CH_2-$\underline{CH}$-CH_2 (G2), CH-$\underline{CH_2}$-O (G1), CH_2-$\underline{CH_2}$-COO (C2), and $\underline{CH_2}$-CH_2-COO (C3).

In some cases (Figure 5), we observe discontinuities of relative cross-peak volumes for contacts around the G1 lipid protons. The α resonance coincides with one of the proton signals of G1 (Figure 3) (*34*). Therefore, the number of lipid protons by which the volumes of cross-peaks have to be corrected does not necessarily reflect the number of lipid protons actually contributing to the lipid−drug interaction.

The main purpose of this paper was to investigate the membrane interaction of the neutral form of all drugs in pure D_2O. Control experiments on doxorubicin which bears a single positive charge in its daunosamine moiety at pH 7.4 did show a very similar location profile as shown in Figure 5 (see the Supporting Information). We have also altered surface charge and temperature to investigate their effect upon membrane distributions of chloramphenicol, nicardipine, penicillin G, and quinidine. Charged model membranes were prepared by mixing anionic DMPG with DMPC (3:7). At this DMPG:DMPC ratio, the membrane is almost saturated with negative charges (*46*). Our measurements show that the addition of anionic lipids to the model

membrane causes no significant change in the overall location probability for all studied drugs (see the Supporting Information).

Further experiments at a higher temperature (313 K) with chloramphenicol, nicardipine, penicillin G, and quinidine lipid mixtures were carried out. The higher temperature causes shorter lipid and drug correlation times and influences the motional characteristics of lipid−drug interactions. As expected, the relative cross-peak volumes dramatically decreased as correlation times are reduced at higher temperatures (*34*). A smoothed drug distribution might be expected as membrane fluidity also rises with temperature, thus facilitating drug diffusion within the lipid matrix. Experiments at 313 K also present a more physiological situation. However, we observed no change in the resulting drug location probability within the membrane.

DISCUSSION

Our data clearly indicate that all tested drugs accumulate within the membrane, in accord with their high octanol−water partition coefficients (Table 1). The relative lipid−drug cross-peak volumes shown in Figure 5 offer direct evidence of the preferred interfacial location of the aromatic groups of all nine drugs, although their distribution across the hydrophobic core region is less well defined. Protons from each CH_2 chain segment have the same chemical shift but could contribute differently to each cross-peak volume due to different contacts with the substrate. A better spatial resolution is offered by other NMR approaches such as ^2H NMR on selectively chain deuterated lipids or ^{13}C MAS NMR, as demonstrated for the antidepressants desipramine and imipramine (also PGP substrates). They have been found to show contacts down to the sixth of 14 carbons on the lipid acyl chain (*26*, *47*). However, there is no doubt that the aromatic groups of all nine tested drugs shown in Figure 2 have a preferred equilibrium location within the interface region, i.e., within a narrow layer between upper segments of the lipid acyl chain and below the phosphate of the lipid headgroup (Figure 5).

Drug−Membrane Interactions. The main reason for this distribution is a balanced interplay between hydrophobic and electrostatic effects. Lipid membranes are characterized by a steep hydrophobicity profile with dielectricity constants ranging from 80 at the aqueous phase to 2 inside the hydrocarbon phase (*48*) as well a strong electric dipole potential (*49*). The drugs used in his study contain both hydrophilic and hydrophobic groups. They are weak bases or acids which remain mainly uncharged under the conditions used here (*50*). Therefore, only their π-electron systems and to a lesser extent electric dipole and quadrupole moments would weakly contribute to electrostatic interactions with the dipole of the zwitterionic DMPC lipid headgroup (*33*). In addition, the formation of hydrogen bonds between the lipid carbonyls and drug molecules supports a preferred location within the membrane interface (*49*, *51*). Therefore, hydrophobic substances would have a preference for the membrane core region, while electrostatic interactions would cause a preference for the lipid headgroups. These effects could offset each other in the interface region.

Four of the drugs (doxorubicin, quinidine, penicillin G, and ampicillin) used here have already been investigated with respect to their interaction with lipids. Studies on quinidine and its optical isomer quinine have shown that it interacts with both neutral and charged lipids. However, penetration into the bilayer has only been observed in the presence of charged lipids (DMPG) (*52*). Ampicillin (*53*) and penicillin G (*54*) have been found to interact with model membranes as well, but spatially resolved details could not be obtained.

Anthracyclines, and especially doxorubicin, have been subjected to especially intense scrutiny by a variety of methods in both neutral and anionic lipids (*55*). Membrane binding involves a complex interplay of both hydrophobic and electrostatic interactions. Using NMR, it was found that it interacts with both surface and buried sites in bicelles containing DMPC and cardiolipin (*55*), while monolayer studies showed no penetration into the hydrophobic region of the membrane. It has been shown that the presence of anionic lipids increases the strength of binding of doxorubicin to the bilayers (*56*) but slows passive transport through the membrane (*57*). Interestingly, some fluorescence studies have suggested two binding environments in PC/cardiolipin bilayers (*58*). While our studies have focused on the detailed location of the neutral form of doxorubicin within zwitterionic lipids, our data also show a preferred interaction with the interface region. Doxorubicin does not penetrate deeply into the hydrophobic core. Indeed, Figure 5B indicates two maxima for the location probability, one more exposed between water and the lipid headgroup and a second between the lipid headgroup and the hydrophobic core region of the lipids.

At physiological pH (7.4), 94% of the doxorubicin molecules bear a positive charge at the daunosamine group ($pK_a = 8.4$), leading to strong electrostatic binding to anionic lipids. However, it is the uncharged form of the drug which is transported via passive diffusion across the membranes (*59*), and it has also been shown that it is transported better by PGP than charged doxorubicin (*21*). Our data show a very similar location profile of neutral doxorubicin (Figure 5B) compared to that for data acquired at pH 7.4 (see the Supporting Information). This is consistent which fluorescence studies which did show that drug incorporation in the bilayer does not depend on the presence of a positive charge or on anionic lipids but on the hydrophobicity of the molecule (*60*).

Comparison with Physiological Conditions. Under physiological conditions, the total lipid:drug ratio in cell membranes is significantly lower than the ratios used in our measurements. Our use of higher ratios was a requirement due to the low signal-to-noise ratio of the observed drug resonances. However, line width and chemical shifts of lipid resonances did not change significantly compared to those of drug-free liposomes, indicating an intact bilayer structure. Indeed, we note that previously published studies used comparable drug:lipid ratios (*27*, *33*). Although our major goal was a comparative study of the interaction of nine PGP substrates or modulators with neutral/zwitterionic lipids, the effect of charged lipids (7:3 DMPC:DMPG ratio) on the drug distribution within the membrane was additionally studied, due to the importance of charged lipids for drug−membrane interactions. The locations of chloramphenicol, nicardipine, penicillin G, and quinidine within the DMPC/DMPG membrane were evaluated. No qualitative change was observed when compared with DMPC membranes. This result, and

the fact that substrate−PGP binding affinity has been shown to be higher in DMPC than in PS or PE, indicate that DMPC is a good choice as a model system (*23*).

Relevance of Our Findings for Passive Uptake Models. Due to their mainly lipophilic nature, most drugs "dissolve" and accumulate within the membrane. In contrast to active efflux, drug uptake takes place by passive diffusion across the membrane along the drug concentration gradient. The high substrate concentration in the interface region found here supports the model of a three-step process for the drug to cross the membrane. (i) Substrate accumulates in the interface of the outer leaflet, and (ii) it flips over to the interface of the inner leaflet and (iii) is found to be in equilibrium with the intracellular space. Therefore, our findings support the previously suggested flip-flop model for passive drug uptake (*61*, *62*).

Relevance of Our Findings for Efflux. Although the binding sites for hydrophobic substrates are assumed to be in the transmembrane region, their exact location is not yet known despite a number of studies using mutagenesis, photoaffinity labeling, and fluorescence spectroscopy (*11*, *12*, *15*, *20*, *63*−*65*). An important role of aromatic residues for substrate binding has been suggested (*4*, *17*), and indeed, a common building block of the rather diverse set of substrates is the aromatic ring structure (*20*). In this case, drug binding could take place via π−cation and stacking interactions with aromatic and polar amino acids present in the transmembrane domain of PGP and LmrA (*20*, *65*, *66*). Aromatic residues in membrane proteins are likely to be exposed to the membrane interface region (*67*), where the substrates studied here have their highest concentrations. Interestingly, the relatively low binding affinity of many PGP substrates (micromolar) increases with an increase in the membrane partition coefficient (*68*). This means that an increasing substrate concentration in the membrane is needed for efficient binding. Therefore, our data support a model in which drug binding sites are located within or accessible from the membrane interface (*15*).

We have included in our study not only PGP substrates (Table 1) but also the two modulators nicardipine and quinidine (*4*), which have been found to decrease PGP activity (*69*). Interestingly, we have found no differences in the membrane location for substrates and modulators. This could indicate that substrates and modulators enter the proteins via similar pathways or that substrate and modulator binding sites are both accessible from the membrane interface. The high degrees of similarity in structure, partition coefficient, and membrane interaction between substrates and modulators may make it very difficult to define molecular properties needed to eventually design a potent inhibitor.

Existing transport models imply that bound substrates are taken up from the inner leaflet, moved across the membrane, and released either into the outer leaflet (flippase model) or directly into the extracellular space (hydrophobic vacuum cleaner model). Although substrate−lipid interactions and their well-defined membrane location found here can be related to drug uptake and binding, it is difficult to draw any conclusions about their translocation and release. Their preference for the interface region makes a flippase model likely. In this case, the transporter would have to flip drugs at a rate higher than that of flip-flops observed during passive uptake. In contrast, the existence of an aqueous transmembrane chamber open to the extracellular milieu as suggested for PGP or LmrA could also serve to release bound substrates directly (*7*, *8*, *64*).

CONCLUSIONS AND PERSPECTIVE

ABC efflux pumps such as P-glycoprotein provide an important but not yet understood multidrug resistance mechanism for protecting cells against poisonous chemicals in the environment. In this study, the location of seven PGP substrates and two modulators within neutral phospholipid bilayers was examined by NOESY MAS NMR. Although structurally rather diverse, all molecules show a very similar behavior within the membrane and are found predominantly within the membrane interface region but are less likely to penetrate into the membrane's hydrophobic core region.

Furthermore, both substrates and modulators exhibit a similar membrane location profile. Therefore, substrate and modulator binding sites in PGP are most likely accessible from within the interface region. These findings might also have relevance for the understanding of secondary multidrug efflux pumps due to their partially overlapping substrate specificity and their ability to bind substrates from within the membrane as shown, for example, for LmrP (*70*).

An obvious next step would be to perform more detailed drug−protein interaction studies to obtain molecular details about the substrate and modulator binding pockets. One suitable approach would be solid-state NMR on the labeled transporter in complex with labeled substrates. For example, the PGP functional homologue in *L. lactis* LmrA has been shown to be suitable for isotope labeling and high-level reconstitution into phospholipids (*71*), offering a realistic perspective for such studies.

ACKNOWLEDGMENT

We thank Dr. M. Lorch for comments on the manuscript.

SUPPORTING INFORMATION AVAILABLE

Evaluation of the NOESY MAS NMR approach (Figure S1), normalized DMPC−substrate cross-peak volumes for all protons analyzed (Figure S2), substrate location in mixed DMPC/DMPG vesicles (Figure S3), and comparison of proton 3 in doxorubicin and proton 2 in chloramphenicol buffered at pH 7.4 (Figure S4). This material is available free of charge via the Internet at http://pubs.acs.org.

REFERENCES

1. Brennan, R. G. (2001) Introduction: Multidrug resistance, *Semin. Cell Dev. Biol. 12*, 201−204.
2. Blackmore, C. G., McNaughton, P. A., and van Veen, H. W. (2001) Multidrug transporters in prokaryotic and eukaryotic cells: Physiological functions and transport mechanisms, *Mol. Membr. Biol. 18*, 97−103.
3. Saier, M. H., Paulsen, I. T., Sliwinski, M. K., Pao, S. S., Skurray, R. A., and Nikaido, H. (1998) Evolutionary origins of multidrug and drug-specific efflux pumps in bacteria, *FASEB J. 12*, 265−274.
4. Ambudkar, S. V., Kimchi-Sarfaty, C., Sauna, Z. E., and Gottesman, M. M. (2003) P-glycoprotein: From genomics to mechanism, *Oncogene 22*, 7468−7485.
5. Higgins, C. F., and Gottesman, M. M. (1992) Is the Multidrug Transporter a Flippase, *Trends Biochem. Sci. 17*, 18−21.
6. van Veen, H. W., Callaghan, R., Soceneantu, L., Sardini, A., Konings, W. N., and Higgins, C. F. (1998) A bacterial antibiotic-

resistance gene that complements the human multidrug-resistance P-glycoprotein gene, *Nature 391*, 291−295.
7. Rosenberg, M. F., Callaghan, R., Ford, R. C., and Higgins, C. F. (1997) Structure of the multidrug resistance P-glycoprotein to 2.5 nm resolution determined by electron microscopy and image analysis, *J. Biol. Chem. 272*, 10685−10694.
8. Poelarends, G. J., and Konings, W. N. (2002) The transmembrane domains of the ABC multidrug transporter LmrA form a cytoplasmic exposed, aqueous chamber within the membrane, *J. Biol. Chem. 277*, 42891−42898.
9. Ueda, K., Taguchi, Y., and Morishima, M. (1997) How does P-glycoprotein recognize its substrates? *Cancer Biol. 8*, 151−159.
10. Langton, K. P., Henderson, P. J. F., and Herbert, R. B. (2005) Antibiotic resistance: Multidrug efflux proteins, a common transport mechanism? *Nat. Prod. Rep. 22*, 439−451.
11. Loo, T. W., Bartlett, M. C., and Clarke, D. M. (2004) The drug-binding pocket of the human multidrug resistance P-glycoprotein is accessible to the aqueous medium, *Biochemistry 43*, 12081−12089.
12. Loo, T. W., Bartlett, M. C., and Clarke, D. M. (2004) Processing mutations located throughout the human multidrug resistance P-glycoprotein disrupt interactions between the nucleotide binding domains, *J. Biol. Chem. 279*, 38395−38401.
13. Peer, M., Csaszar, E., Vorlaufer, E., Kopp, S., and Chiba, P. (2005) Photoaffinity labeling of P-glycoprotein, *Mini-Rev. Med. Chem. 5*, 165−172.
14. Pleban, K., Kopp, S., Csaszar, E., Peer, M., Hrebicek, T., Rizzi, A., Ecker, G., and Chiba, P. (2005) P-Glycoprotein substrate binding domains are located at the transmembrane domain/transmebrane domain interface: A combined photoaffinity labeling-protein homology modeling approach, *Mol. Pharmacol. 67*, 365−374.
15. Lugo, M. R., and Sharom, F. J. (2005) Interaction of LDS-751 with P-glycoprotein and mapping of the location of the R drug binding site, *Biochemistry 44*, 643−655.
16. Shapiro, A. B., and Ling, V. (1998) Transport of LDS-751 from the cytoplasmic leaflet of thr plasma membrane by ther rhodamine-123-selective site of P-glycoprotein, *Eur. J. Biochem. 254*, 181−188.
17. Pawagi, A. B., Wang, J., Silverman, M., Reithmeier, R. A., and Deber, C. M. (1994) Transmembrane aromatic amino acid distribution in P-glycoprotein. A functional role in broad substrate specificity, *J. Mol. Biol. 235*, 554−564.
18. Onishi, Y., Hirano, H., Nakata, K., Oosumi, K., Nagakura, M., Tarui, S., and Ishikawa, T. (2003) High-speed screening and structure-activity relationship analysis for the substrate specificity of P-glycoprotein, *Chem-Bio Inf. J. 3*, 175−193.
19. Klopman, G., Shi, L. M., and Ramu, A. (1997) Quantitative structure−activity relationship of multidrug resistance reversal agents, *Mol. Pharmacol. 52*, 323−334.
20. Seelig, A., and Landwojtowicz, E. (2000) Structure−activity relationship of P-glycoprotein substrates and modifiers, *Eur. J. Pharm. Sci. 12*, 31−40.
21. Frezard, F., Pereira-Maia, E., Quidu, P., Priebe, W., and Garnier-Suillerot, A. (2001) P-Glycoprotein preferentially effluxes anthracyclines containing free basic versus charged amine, *Eur. J. Biochem. 268*, 1561−1567.
22. Poelarends, G. J., Mazurkiewicz, P., Putman, M., Cool, R. H., van Veen, H. W., and Konings, W. N. (2000) An ABC-type multidrug transporter of *Lactococcus lactis* possesses an exceptionally broad substrate specificity, *Drug Resist. Updates 3*, 330−334.
23. Romsicki, Y., and Sharom, F. J. (1999) The membrane lipid environment modulates drug interactions with the P-glycoprotein multidrug transporter, *Biochemistry 38*, 6887−6896.
24. Wesolowska, O., Hendrich, A. B., Motohashi, N., Kawase, M., Dobryszycki, P., Ozyhar, A., and Michalak, K. (2004) Presence of anionic phospholipids rules the membrane localization of phenothiazine type multidrug resistance modulator, *Biophys. Chem. 109*, 399−412.
25. Maswadeh, H., Demetzos, C., Daliani, I., Kyrikou, I., Mavromoustakos, T., Tsortos, A., and Nounesis, G. (2002) A molecular basis for explanation of the dynamic and thermal effects of vinblastine sulfate upon dipalmitoylphosphatidylcholine bilayer membranes, *Biochim. Biophys. Acta 1567*, 49−55.
26. Santos, J. S., Lee, D. K., and Ramamoorthy, A. (2004) Effects of antidepressants on the conformation of phospholipid headgroups studied by solid-state NMR, *Magn. Reson. Chem. 42*, 105−114.
27. Scheidt, H. A., Pampel, A., Nissler, L., Gebhardt, R., and Huster, D. (2004) Investigation of the membrane localization and distribution of flavonoids by high-resolution magic angle spinning NMR spectroscopy, *Biochim. Biophys. Acta 1663*, 97−107.
28. Middleton, D. A., Hughes, E., and Madine, J. (2004) Screening molecular associations with lipid membranes using natural abundance C-13 cross-polarization magic-angle spinning NMR and principal component analysis, *J. Am. Chem. Soc. 126*, 9478−9479.
29. Bäuerle, H.-D., and Seeling, J. (1991) Interaction of charged and uncharged calcium channel antagonists with phospholipid membranes. Binding equilibrium, binding enthalpy, and membrane location, *Biochemistry 30*, 7203−7211.
30. Schote, U., and Seelig, J. (1998) Interaction of the neuronal marker dye FM1−43 with lipid membranes: Thermodynamics and lipid ordering, *Biochim. Biophys. Acta 1415*, 135−146.
31. Pedros, J., Porcar, I., Gomez, C. M., Campos, A., and Abad, C. (1997) Interaction of quinidine with negatively charged lipid vesicles studied by fluorescence spectroscopy. Influence of the pH., *Spectrochim. Acta, Part A 53*, 421−431.
32. Huster, D., Vogel, A., Katzka, C., Scheidt, H. A., Binder, H., Dante, S., Gutberlet, T., Zschörnig, O., Waldmann, H., and Arnold, K. (2003) Membrane insertion of a lipidated Ras peptide studied by FTIR, solid-state NMR, and neuron diffraction spectroscopy, *J. Am. Chem. Soc. 125*, 4070−4079.
33. Yau, W. M., Wimley, W. C., Gawrisch, K., and White, S. H. (1998) The preference of tryptophan for membrane interfaces, *Biochemistry 37*, 14713−14718.
34. Holte, L. L., and Gawrisch, K. (1997) Determining ethanol distribution in phospholipid multilayers with MAS-NOESY spectra, *Biochemistry 36*, 4669−4674.
35. Huster, D., Arnold, K., and Gawrisch, K. (1999) Investigation of lipid organization in biological membranes by two-dimensional nuclear overhauser enhancement spectroscopy, *J. Phys. Chem. B 103*, 243−251.
36. Ellena, J. F., Dominey, R. N., Archer, S. J., Xu, Z. C., and Cafiso, D. S. (1987) Localization of Hydrophobic Ions in Phospholipid-Bilayers Using H-1 Nuclear Overhauser Effect Spectroscopy, *Biochemistry 26*, 4584−4592.
37. Yokono, S., Ogli, K., Miura, S., and Ueda, I. (1989) 400 MHz Two-Dimensional Nuclear Overhauser Spectroscopy on Anesthetic Interaction with Lipid Bilayer, *Biochim. Biophys. Acta 982*, 300−302.
38. Van Bambeke, F., Balzi, E., and Tulkens, P. M. (2000) Antibiotic efflux pumps: Commentary, *Biochem. Pharmacol. 60*, 457−470.
39. Varma, M. V. S., Ashokraj, Y., Dey, C. S., and Panchagnula, R. (2003) P-Glycoprotein inhibitors and their screening: A perspective from bioavailability enhancement, *Pharmacol. Res. 48*, 347−359.
40. Tung, J. C., Gonzales, A. J., Sadowsky, J. D., and O'Leary, D. J. (2000) On the H-1 NMR chemical shift assignments for ampicillin, *Magn. Reson. Chem. 38*, 126−128.
41. Zolek, T., Paradowska, K., Krajewska, D., Rozanski, A., and Wawer, I. (2003) H-1, C-13 MAS NMR and GIAO-CPHF calculations of chloramphenicol, thiamphenicol and their pyrrole analogues, *J. Mol. Struct. 646*, 141−149.
42. Calzolai, L., Gaggelli, E., Maccotta, A., and Valensin, G. (1997) Nuclear magnetic resonance investigations of calcium-antagonist drugs. 4. Conformational and dynamic features of nicardipine {methyl 2-methyl(phenylmethyl)amino ethyl 1,4-dihydro-2,6-dimethyl-4-(3-nitrophenyl)pyridine-3,5-dicarboxylate} in deuterium oxide, *J. Chem. Soc., Perkin Trans. 2*, 363−367.
43. Gaggelli, E., Valensin, G., Stolowich, N. J., Williams, H. J., and Scott, A. I. (1992) Conformation of Vinblastine in Aqueous-Solution Determined by 2D H-1-NMR and C-13-NMR Spectroscopy, *J. Nat. Prod. 55*, 285−293.
44. Garipova, I. Y., and Silnikov, V. N. (2003) New synthetic approaches to multifunctional phenazinium salt derivatives, *Molecules 8*, 505−519.
45. Lindholm, A., Mäki-Arvela, P., Toukoniitty, E., Pakkanen, T. Y., Hirvi, J. T., Salmi, T., Murzin, D. Y., Sjöholm, R., and Leino, R. (2002) Hydrosilytion of cinchonidine and 9-O-TMS-cinchonidine with triethoxysilane: application of 11-(triethoxysilyl)-10,11-dihydrocinchonidine as a chiral modifier in the enantioselective hydrogenation of 1-phenylpropane-1,2-dione, *J. Chem. Soc., Perkin Trans. 1*, 2605−2612.
46. Wiedmer, S. K., Hautala, J., Holopainen, J. M., Kinnunen, P. K. J., and Riekkola, M. L. (2001) Study on liposomes by capillary electrophoresis, *Electrophoresis 22*, 1305−1313.

47. Meadows, M. D. (1979) Ph.D. Thesis, University of Illinois, Urbana, IL.
48. Subczynski, W. K., Wisniewska, A., Yin, J.-J., Hyde, J. S., and Kusumi, A. (1994) Hydrophobic barriers of lipid bilayer membranes formed by reduction of water penetration by alkyl chain saturation and cholesterol, *Biochemistry 33*, 7670−7681.
49. Clarke, R. J. (2001) The dipole potential of phospholipid membranes and methods for its detection, *Adv. Colloid Interface Sci. 89*−*90*, 263−281.
50. Ferte, J. (2000) Analysis of tangled relationships between P-glycoprotein-mediated multidrug resistance and the lipid phase of the cell membrane, *Eur. J. Biochem. 267*, 277−294.
51. Castaing, M., Loiseau, A., and Mullliert, G. (2005) Multidrug resistance modulator interactions with neutral and anionic liposomes: Membrane binding affinity and membrane perturbing activity, *J. Pharm. Pharmacol. 57*, 547−554.
52. Porcar, I., Codoner, A., Gomez, C. M., Abad, C., and Campos, A. (2003) Interaction of quinine with model lipid membranes of different compositions, *J. Pharm. Sci. 92*, 45−57.
53. Casa, M., Boissonnade, M. M., and Baszkin, A. (1992) Penetration of chlorcyclizine and ampicillin into mixed phospholipid-oleic acid monolayers, *Colloid Surf. 68*, 207−214.
54. Suwalsky, M., Villena, F., Aguilar, F., and Sotomayor, C. P. (1996) Interaction of penicillin G with the human erythrocyte membrane and models, *Z. Naturforsch. 51c*, 243−248.
55. Parker, M. A., King, V., and Howard, K. P. (2001) Nuclear magnetic resonance study of doxorubicin binding to cardiolipin containing magnetically oriented phospholipid bilayers, *Biochim. Biophys. Acta 1514*, 206−216.
56. de Wolf, F. A., Demel, R. A., Bets, D., Vankats, C., and de Kruijff, B. (1991) Characterization of the Interaction of Doxorubicin with (Poly)Phosphoinositides in Model Systems: Evidence for Specific Interaction with Phosphatidylinositol-Monophosphate and Phosphatidylinositol-Diphosphate, *FEBS Lett. 288*, 237−240.
57. Speelmans, G., Staffhorst, R. W. H. M., Dekruijff, B., and Dewolf, F. A. (1994) Transport Studies of Doxorubicin in Model Membranes Indicate a Difference in Passive Diffusion across and Binding at the Outer and Inner Leaflets of the Plasma-Membrane, *Biochemistry 33*, 13761−13768.
58. Karczmar, G. S., and Tritton, T. R. (1979) Interaction of adryamycin with small unilamellar vesicle liposomes: Fluorescence study, *Biochim. Biophys. Acta 557*, 306−319.
59. Frezard, F., and Garniersuillerot, A. (1991) DNA-Containing Liposomes as a Model for the Study of Cell-Membrane Permeation by Anthracycline Derivatives, *Biochemistry 30*, 5038−5043.
60. Gallois, L., Fiallo, M., Laigle, A., Priebe, W., and GarnierSuillerot, A. (1996) The overall partitioning of anthracyclines into phosphatidyl-containing model membranes depends neither on the drug charge nor the presence of anionic phospholipids, *Eur. J. Biochem. 241*, 879−887.
61. Eytan, G. D., Regev, R., Oren, G., and Assaraf, Y. G. (1996) The role of passive transbilayer drug movement in multidrug resistance and its modulation, *J. Biol. Chem. 271*, 12897−12902.
62. Eytan, G. D. (2005) Mechanism of multidrug resistance in relation to passive membrane permeation, *Biomed. Pharmacother. 59*, 90−97.
63. Loo, T. W., and Clarke, D. M. (2001) Determining the dimensions of the drug-binding domain of human P-glycoprotein using thiol cros-linking compounds as molecular rulers, *J. Biol. Chem. 276*, 36877−36880.
64. Loo, T. W., Bartlett, M. C., and Clarke, D. M. (2003) Substrate-induced conformational, changes in the transmembrane segments of human P-glycoprotein: Direct evidence for the substrate-induced fit mechanism for drug binding, *J. Biol. Chem. 278*, 13603−13606.
65. Dougherty, D. A. (1996) Cation-π interactions in chemistry and biology: A new view of benzene, Phe, Tyr, and Trp, *Science 271*, 163−168.
66. van Veen, H. W. (2001) Towards the molecular mechanism of prokaryotic and eukaryotic multidrug transporters, *Semin. Cell Dev. Biol. 12*, 239−245.
67. von Heijne, G. (1992) Membrane protein structure prediction. Hydrophobicity analysis and the positive-inside rule, *J. Mol. Biol. 225*, 487−494.
68. Sharom, F. J., Liu, R. H., Romsicki, Y., and Lu, P. H. (1999) Insights into the structure and substrate interactions of the P-glycoprotein multidrug transporter from spectroscopic studies, *Biochim. Biophys. Acta 1461*, 327−345.
69. Wang, E.-J., Casciano, C. N., Clement, R. P., and Johnson, W. W. (2000) In Vitro Flow Cytometry Method to Quantitatively Assess Inhibitors of P-Glycoprotein, *Drug Metab. Dispos. 28*, 522−528.
70. Bolhuis, H., van Veen, H. W., Molenaar, D., Poolman, B., Driessen, A. J. M., and Konings, W. N. (1996) Multidrug resistance in *Lactococcus lactis*: Evidence for ATP-dependent drug extrusion from the inner leaflet of the cytoplasmic membrane, *EMBO J. 15*, 4239−4245.
71. Mason, A. J., Siarheyeva, A., Haase, W., Lorch, M., van Veen, H., and Glaubitz, C. (2004) Amino acid type selective isotope labelling of the multidrug ABC transporter LmrA for solid-state NMR studies, *FEBS Lett. 568*, 117−121.
72. *Advanced Chemistry Development (ACD/Labs) Software Solaris*, version 4.67 (1994−2005) ACD/Labs.
73. Van't Land, C. W., Mocek, U., and Floss, H. G. (1993) Biosynthesis of the phenazine antibiotics, the Saphenamycins and Esmeraldins, in *Streptomyces antibioticus*, *J. Org. Chem. 58*, 6576−6582.
74. Pinciroli, V., Rizzo, V., Angelucci, F., Tato, M., and Vigevani, A. (1997) ^{1}H NMR characterization of methacrylamide polymer conjugates with the anti-cancer derug doxorubicin, *Magn. Reson. Chem. 35*, 2−8.
75. Bartzatt, R., and Malesa, C. (2003) Synthesis, structural analysis and antibacterial activity of a butyl ester derivative of ampicillin, *Chemotherapy 49*, 213−221.

BI0524870